

## Two-photon decay of $2^1S_0$ and $2^3S_1$ states of heliumlike ions

A. Derevianko and W. R. Johnson

*Department of Physics, Notre Dame University, Notre Dame, Indiana 46556*

(Received 18 February 1997)

Systematic calculations of two-photon decay rates of metastable  $2^1S_0$  and  $2^3S_1$  states are presented for heliumlike ions with nuclear charges in the range  $Z=2-100$ . These calculations include retardation and are carried out using relativistic configuration-interaction wave functions that account for the Breit interaction. Photon energy distributions and total rates are given. The relativistic  $2^1S_0$  decay rates agree, to within two standard deviations, with precise measurements for heliumlike Ar, Ni, Br, Kr, and Nb. The calculated  $2^1S_0$  rates are 30% smaller than the corresponding nonrelativistic rates at high  $Z$ . The  $2^3S_1$  two-photon decay rates remain a factor of about  $10^{-4}$  of the corresponding  $M1$  rates throughout the helium isoelectronic sequence. [S1050-2947(97)07808-6]

PACS number(s): 31.10.+z, 31.30.Jv, 32.70.Cs, 32.80.-t

### I. INTRODUCTION

In this paper, we evaluate two-photon decay rates for  $2^1S_0$  and  $2^3S_1$  states of heliumlike ions. Our calculations are carried out using relativistic wave functions that account for the Breit interaction and include retardation of the dipole transition operator. The first theoretical two-photon decay rate for the  $2^1S_0$  state for helium was given by Dalgarno [1]. In the 30 years since Ref. [1] was published, a number of increasingly sophisticated nonrelativistic calculations of the  $2^1S_0$  decay rate have been carried out for helium and for light heliumlike ions by Dalgarno and Victor [2], Victor [3], Victor and Dalgarno [4], Drake, Victor, and Dalgarno [5], and by Jacobs [6]. A decade ago, Drake [7] gave highly accurate nonrelativistic values of two-photon decay rates of  $2^1S_0$  states for heliumlike ions with nuclear charges  $Z$  from 2 to 92, and estimated relativistic corrections to these rates. Calculations of two-photon decay rates for  $2^3S_1$  states of heliumlike ions were made by Bely [8], Bely and Faucher [9], Drake and Dalgarno [10], and Drake, Victor, and Dalgarno [5]. These two-photon rates are smaller than the corresponding single-photon  $M1$  decay rates for the  $2^3S_1$  state by a factor of about  $10^{-4}$ . Both one- and two-photon transitions from the  $2^3S_1$  excited state to the  $1^1S_0$  ground state are sensitive to relativistic corrections.

Precise measurements of lifetimes of metastable  $2^1S_0$  states of He and  $\text{Li}^+$  have been reported in Refs. [11,12]. In the recent past, measurements of lifetimes of metastable  $2^1S_0$  states of heliumlike ions have been extended to include  $\text{Ar}^{+16}$  [13,14],  $\text{Ni}^{+26}$  [15-17],  $\text{Br}^{+33}$  [18],  $\text{Kr}^{+34}$  [14], and  $\text{Nb}^{+39}$  [19]. A measurement of the photon energy distribution for the  $2^1S_0$  decay has also been reported recently for heliumlike  $\text{Kr}^{+34}$  [20,21]. One goal of the recent measurements was to determine the size of relativistic corrections to two-photon decay rates. The aim of the present paper is to provide accurate relativistic predictions of two-photon decay rates and photon energy distributions for comparisons with such experiments.

The wave functions used in this calculation are determined from a variational principle, seeking extrema of the expectation value of the *no-pair* Hamiltonian including both

the Coulomb and Breit interactions. Discussions of the relativistic configuration-interaction (CI) problem for heliumlike ions including extensive comparisons of CI energies with experiment have been given in Refs. [22,23]. Relativistic CI wave functions have been used previously to evaluate single-photon decay rates in heliumlike ions in Ref. [24]. The method used here to evaluate the sum over intermediate states in the two-photon matrix element is similar to that used in a recent study of relativistic corrections to polarizabilities of heliumlike ions [25].

In the present calculation, we give relativistic two-photon rates for ions with nuclear charges  $Z = 2-20, 25, 30, \dots, 100$ , and for the special cases  $Z = 28, 36, 41, 54, 82$ , and 92. We also study the  $Z$  dependence of the photon energy distribution. The full width at half maximum (FWHM) of the photon energy distribution increases with nuclear charge as  $Z^2$ . We introduce a reduced photon energy variable  $y = \omega/\omega_0$ ,  $\omega_0$  being the maximum photon energy, and a corresponding reduced FWHM measured in terms of  $y$ . We find that the reduced FWHM of the  $2^1S_0$  energy distribution increases with  $Z$  from 2 to 20 then decreases steadily to  $Z=100$ . By contrast, the reduced FWHM of the  $2^3S_1$  distribution decreases from 2 to 30 and then increases from  $Z = 30$  to 100. Relativistic corrections to the  $2^1S_0$  rate, inferred by comparing the present calculations with precise nonrelativistic values from [7], are found to be in fair agreement with relativistic corrections estimated in Ref. [7]. The values of the present  $2^1S_0$  rates are also in good agreement with available experimental measurements.

### II. THEORY

The probability per unit time for a transition from state  $\Psi_I$  to state  $\Psi_F$  with the emission of two  $E1$  photons,  $\omega_1$  and  $\omega_2$ , is

$$dw_{FI} = \frac{8}{9\pi} \alpha^6 \omega_1^3 \omega_2^3 d\omega_1 \sum_{M_1 M_2} |M_{M_2 M_1}|^2, \quad (2.1)$$

where

$$M_{M_2M_1} = - \sum_n \left[ \frac{\langle \Psi_I | Q_{M_2} | \Psi_n \rangle \langle \Psi_n | Q_{M_1} | \Psi_F \rangle}{E_n + \omega_2 - E_I} + \frac{\langle \Psi_I | Q_{M_1} | \Psi_n \rangle \langle \Psi_n | Q_{M_2} | \Psi_F \rangle}{E_n + \omega_1 - E_I} \right]. \quad (2.2)$$

In this expression,  $Q_M(k)$  is the retarded electric-dipole operator, which (in second-quantized form) is given by

$$Q_M(k) = \sum_{ij} [q_M(k\mathbf{r})]_{ij} a_i^\dagger a_j. \quad (2.3)$$

Explicit formulas for the single-particle matrix elements  $[q_M(k\mathbf{r})]_{ij}$  in Eq. (2.3) are given in Ref. [24]. In the nonrelativistic limit,  $q_M$  approaches  $r_M$ , the  $M$ th component of the coordinate vector in a spherical basis.

In the present calculation, we assume that the final state  $\Psi_F$  is the  $1^1S_0$  ground state of a two-electron ion and that the initial state  $\Psi_I$  is either a  $2^1S_0$  or a  $2^3S_1$  excited state. The wave functions for these states are obtained from relativistic CI calculations. For the initial (final) state, we write

$$\Psi_{I(F)} = \sum_{k \geq l} c_{kl}^{I(F)} \Phi_{kl}, \quad (2.4)$$

where  $\Phi_{kl}$  are configuration state functions coupled to given values of  $J$ ,  $M$ , and parity. The coefficients and  $c_{kl}^{I(F)}$  are configuration weights for the initial (final) state determined variationally. The configuration state functions  $\Phi_{kl}$  are defined by

$$\Phi_{kl} = \eta_{kl} \sum_{m_k m_l} \langle j_k m_k j_l m_l | JM \rangle a_k^\dagger a_l^\dagger | 0 \rangle, \quad (2.5)$$

where  $\eta_{kl} = 1/\sqrt{2}$  if  $k=l$  and  $\eta_{kl} = 1$ , otherwise. The numerical methods used to evaluate the weight coefficients  $c_{kl}^{I(F)}$  are discussed in [22,23].

We introduce the perturbed wave functions

$$|\delta\Psi_{DM_1}\rangle = \sum_n \frac{|\Psi_n\rangle \langle \Psi_n | Q_{M_1}(k_1) | \Psi_F \rangle}{E_n + \omega_2 - E_I}, \quad (2.6)$$

$$|\delta\Psi_{EM_2}\rangle = \sum_n \frac{|\Psi_n\rangle \langle \Psi_n | Q_{M_2}(k_2) | \Psi_F \rangle}{E_n + \omega_1 - E_I}. \quad (2.7)$$

These wave functions satisfy the inhomogeneous two-electron Dirac equations

$$(H + \omega_2 - E_I) |\delta\Psi_{DM_1}\rangle = Q_{M_1}(k_1) |\Psi_F\rangle, \quad (2.8)$$

$$(H + \omega_1 - E_I) |\delta\Psi_{EM_2}\rangle = Q_{M_2}(k_2) |\Psi_F\rangle. \quad (2.9)$$

The two-photon matrix element can be expressed in terms of the perturbed wave functions as  $M_{M_2M_1} = D_{M_2M_1} + E_{M_2M_1}$ , where

$$D_{M_2M_1} = - \langle \Psi_I | Q_{M_2}(k_2) | \delta\Psi_{DM_1} \rangle, \quad (2.10)$$

$$E_{M_2M_1} = - \langle \Psi_I | Q_{M_1}(k_1) | \delta\Psi_{EM_2} \rangle. \quad (2.11)$$

We expand the perturbed wave function  $\delta\Psi_{DM_1}$  (which has quantum numbers  $J=1$  and  $M=M_1$ ) as

$$\delta\Psi_{DM_1} = \frac{1}{\sqrt{[1]}} \sum_{n>m} d_{nm} \Phi_{nm}(1M_1). \quad (2.12)$$

Substituting this expansion into Eq. (2.8), we find that the expansion coefficients  $d_{nm}$  satisfy the inhomogeneous equations

$$\sum_{n>m} [(\epsilon_n + \epsilon_m + \omega_2 - E_I) \delta_{rn} \delta_{sm} + V_{rs, nm}] d_{nm} = b_{rs}(k_1), \quad (2.13)$$

where

$$b_{rs}(k_1) = \sum_{k \geq l} \frac{\eta_{kl} \delta_{\kappa_k \kappa_l}}{\sqrt{[j_k]}} c_{kl}^F [\langle r || q(k_1) || k \rangle \delta_{ls} + \langle r || q(k_1) || l \rangle \delta_{ks} - \langle k || q(k_1) || s \rangle \delta_{lr} - \langle l || q(k_1) || s \rangle \delta_{kr}], \quad (2.14)$$

and where  $V_{ij,kl}$  are two-particle matrix elements of the sum of the Coulomb and Breit interactions [22]. The direct-matrix element  $D_{M_2M_1}$  can be written as

$$D_{M_2M_1} = (-1)^{1-M_2} \begin{pmatrix} 1 & J_I & 1 \\ -M_2 & M_I & M_1 \end{pmatrix} \sqrt{[J_I]} D_I, \quad (2.15)$$

where  $D_I$  is expressed in terms of the solutions to the inhomogeneous equations  $d_{nm}$  by

$$D_I = \sum_{\substack{i>j \\ r>s}} \eta_{ij} c_{ij}^I d_{rs} \left[ (-1)^{i+s+1} \begin{Bmatrix} J_I & 1 & 1 \\ r & s & i \end{Bmatrix} \delta_{js} \langle i || q(k_2) || r \rangle + (-1)^{i+s} \begin{Bmatrix} J_I & 1 & 1 \\ s & r & i \end{Bmatrix} \delta_{jr} \langle i || q(k_2) || s \rangle \right. \\ \left. + (-1)^{J_I} \begin{Bmatrix} J_I & 1 & 1 \\ r & s & j \end{Bmatrix} \delta_{is} \langle j || q(k_2) || r \rangle + (-1)^{J_I+r+s} \begin{Bmatrix} J_I & 1 & 1 \\ s & r & j \end{Bmatrix} \delta_{ir} \langle j || q(k_2) || s \rangle \right]. \quad (2.16)$$

TABLE I. Convergence pattern of two-photon decay rates  $w(l)$  ( $s^{-1}$ ) for the  $2^1S_0$  states for  $Z = 2$  and 10. The index  $l$  represents the maximum value of angular momentum included in the CI expansion of the initial and final states. The calculated minimum transition wavelengths ( $\text{\AA}$ ) are denoted by  $\lambda_l$ . The rows labeled “ $\infty$ ” give rates obtained by extrapolation. Numbers in brackets represent powers of 10.

$Z$	$l$	$\lambda_l$ ( $\text{\AA}$ )	$w(l)$ ( $s^{-1}$ )
2	0	620.07	4.7056[01]
	1	603.70	5.0220[01]
	2	602.02	5.0788[01]
	3	601.61	5.0921[01]
	4	601.53	5.0968[01]
	$\infty$	601.42	5.1016[01]
10	0	13.554	1.0113[07]
	1	13.545	1.0004[07]
	2	13.544	1.0010[07]
	3	13.544	1.0012[07]
	4	13.544	1.0012[07]
	$\infty$	13.544	1.0013[07]

We may also write

$$E_{M_2M_1} = (-1)^{1-M_1} \begin{pmatrix} 1 & J_l & 1 \\ -M_1 & M_l & M_2 \end{pmatrix} \sqrt{[J_l]} E_l, \quad (2.17)$$

where

$$E_l(k_1, k_2) = D_l(k_2, k_1). \quad (2.18)$$

With the aid of these relations, we find

$$\sum_{M_1M_2} |M_{M_1M_2}|^2 = |D_l + (-1)^{J_l} E_l|^2. \quad (2.19)$$

The above expression shows that the direct and exchange contributions add coherently for  $2^1S_0$ , and incoherently for  $2^3S_1$ . Such behavior leads to much smaller rates for the triplet state, and to a high sensitivity of rates and photon

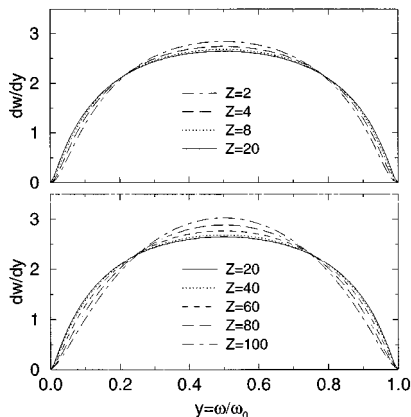


FIG. 1.  $2^1S_0$  state two-photon energy distribution functions  $dw/dy$ , normalized to area 2, are plotted as a function of  $y = \omega/\omega_0$ . The upper panel gives  $dw/dy$  for  $Z \leq 20$  and the lower panel gives results for  $Z \geq 20$ .

TABLE II. Two-photon decay rates  $w_{2\gamma}$  for  $2^1S_0$  states of heliumlike ions. Numbers in brackets are powers of ten.

$Z$	$w_{2\gamma}$ ( $s^{-1}$ )	$Z$	$w_{2\gamma}$ ( $s^{-1}$ )
2	5.102[01]	30	9.938[09]
3	1.940[03]	35	2.540[10]
4	1.816[04]	36	3.012[10]
5	9.211[04]	40	5.692[10]
6	3.300[05]	41	6.604[10]
7	9.444[05]	45	1.154[11]
8	2.310[06]	50	2.164[11]
9	5.029[06]	54	3.415[11]
10	1.001[07]	55	3.806[11]
11	1.856[07]	60	6.350[11]
12	3.249[07]	65	1.013[12]
13	5.421[07]	70	1.556[12]
14	8.685[07]	75	2.312[12]
15	1.344[08]	80	3.336[12]
16	2.020[08]	82	3.834[12]
17	2.957[08]	85	4.690[12]
18	4.230[08]	90	6.439[12]
19	5.930[08]	92	7.265[12]
20	8.163[08]	95	8.653[12]
25	3.249[09]	100	1.140[13]
28	6.517[09]		

energy distributions to relativistic corrections. The expression (2.19), when substituted into Eq. (2.1), gives the formula used here to evaluate the two-photon decay rates.

### III. RESULTS AND CONCLUSIONS

The numerical approach employed here has been used previously in precise calculations of energy levels [22] and polarizabilities [25] of heliumlike ions. As a first step in our calculation, we evaluate the CI wave functions for the initial and final states and obtain the energy separation between transition levels, using methods described in [22,23]. The single-particle basis orbitals used in the CI expansion consist of subsets of 20–30 out of 40  $B$ -spline basis functions for each partial wave. The results were saturated with respect to the number of basis functions. Also we perform a sequence of calculations for the wave functions; the first calculation includes only  $l=0$  ( $s_{1/2}$ ) partial waves, the next includes

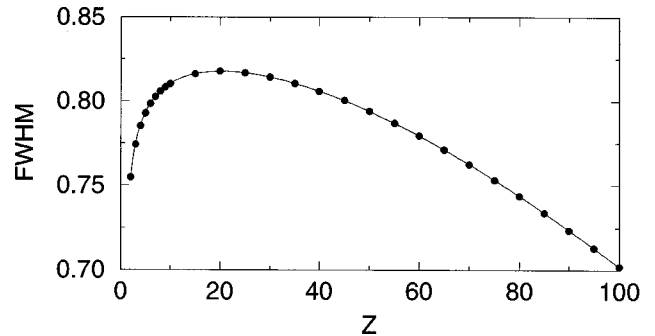


FIG. 2. The reduced full width at half maximum (FWHM) of the two-photon energy distributions  $dw/dy$  for the  $2^1S_0$  state given in Fig. 1 is shown as a function of nuclear charge  $Z$ .

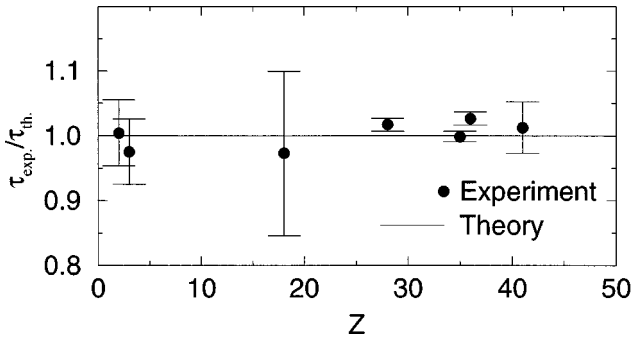


FIG. 3. Ratio of experimental to theoretical lifetimes for  $2^1S_0$  states of He-like ions. The references to experimental data are the same as those given in Table III.

$l=0$  and  $l=1$  ( $s_{1/2}$ ,  $p_{1/2}$ , and  $p_{3/2}$ ) partial waves, and so forth. At each stage, we set up and solve the intermediate state equations (2.13) for  $d_{mn}$ , determine the amplitudes  $D_l$  and  $E_l$  from Eqs. (2.16) and (2.18), and then calculate the differential decay rate. The differential decay rate is evaluated at 100 equally spaced intermediate points; the total rate is determined by numerical integration. The accuracy of the integration was controlled with the Gauss-Kronrod numerical quadrature rule and was found to be better than 1 part in  $10^6$ .

In Table I, we illustrate the convergence pattern of the  $2^1S_0$  decay rate  $w(l)$  for the cases  $Z = 2$  and  $10$  as the number of partial waves  $l$  increases. For  $Z = 2$ , the partial wave sequence converges to about 1 part in  $10^3$  when partial waves with  $l \leq 4$  are included in the initial- and final-state wave functions and partial waves with  $l \leq 5$  are included in the expansion of the perturbed wave function. The convergence improves with increasing  $Z$  so that for  $Z \geq 60$  the partial-wave sequence converges to better than 1 part in  $10^6$  with  $l \leq 3$ . For  $Z \leq 10$  the partial wave sequence  $w(l)$  is extrapolated to infinity, assuming that the incremental changes fall off as  $1/(l+1/2)^n$ . We find  $n \approx 4$ . No extrapolation is necessary for  $Z \geq 10$  to obtain  $2^1S_0$  rates accurate to four figures.

In Table II, we present total two-photon decay rates of  $2^1S_0$  states for all of the cases considered here. These rates grow approximately as  $Z^6$ . The photon energy distributions, expressed as a function of the variable  $y = \omega_1/\omega_0$  (where  $\omega_0 = \omega_1 + \omega_2$ ) are presented for  $Z \leq 20$  in the top panel of Fig. 1, and for  $Z \geq 20$  in the lower panel. These distribution functions are normalized to area 2. The reduced widths of the distributions are seen to increase systematically as  $Z$  in-

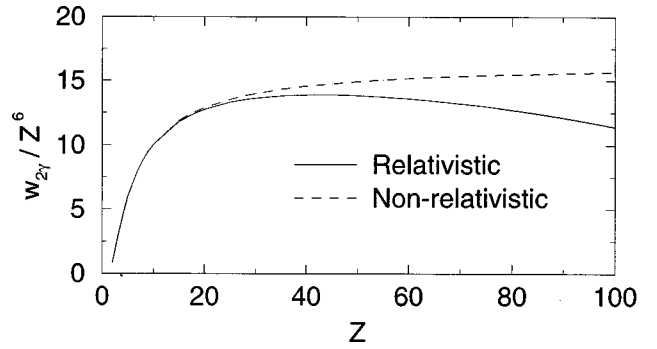


FIG. 4. Comparison of nonrelativistic [7] and relativistic  $2^1S_0$  decay rates,  $w_{2\gamma}(\text{s}^{-1})/Z^6$ .

creases to 20, then decreases as  $Z$  increases from 20 to 100. This behavior is further illustrated in Fig. 2, where the reduced FWHM of the distributions is plotted as a function of  $Z$ . These changes of shape are a consequence of the interplay of correlation and relativity; both effects tend to narrow the energy distribution.

We compare the theoretical and experimental lifetimes  $\tau$  of the  $2^1S_0$  state in Fig. 3 and Table III. The present calculations are seen to be in a good agreement with experimental values; even in the worst cases,  $\text{Kr}^{34+}$  and  $\text{Ni}^{26+}$ , the experimental and theoretical lifetimes differ by only two standard deviations. In Fig. 4, we make a comparison of our relativistic  $2^1S_0$  decay rates with the precise nonrelativistic rates given by Drake [7]. The nonrelativistic calculations overestimate the rate by 30% for high  $Z$ , which demonstrates the importance of *ab initio* relativistic calculations. It should be noted that, for high  $Z$ , Drake's estimated relativistic corrections to  $2^1S_0$  decay rates [7] are in excellent agreement with the values obtained here. The comparison of our results with those of Drake [7] at low  $Z$  are given in Table IV. The values from Ref. [7] tabulated in Table IV include estimated relativistic corrections. The relative difference is found to be less than 1%. For helium, Jacobs [6] gives the decay rate of  $50.85 \text{ s}^{-1}$  and the value of Drake *et al.* [5] is  $51.3 \text{ s}^{-1}$ . Our value for helium ( $51.02 \text{ s}^{-1}$ ) is in a good agreement with the previous results.

Since correlation effects become less important with increasing nuclear charge, one could expect hydrogenlike behavior at large  $Z$ . In Fig. 5 we present the comparison of the photon energy distributions of  $2^1S_0$  decay with the corresponding hydrogenic  $2s_{1/2} \rightarrow 1s_{1/2}$  distributions [26]. This analysis shows that, indeed, the normalized photon energy distributions are virtually indistinguishable for  $Z=92$ . The

TABLE III. Comparison of theoretical lifetimes  $\tau(\text{s})$  of  $2^1S_0$  states of heliumlike ions with experimental values.

$Z$	$\tau$	$\tau_{\text{expt.}}$	Ref.
2	$1.960 \times 10^{-2}$	$1.97(0.10) \times 10^{-2}$	[11]
3	$5.155 \times 10^{-4}$	$5.03(0.26) \times 10^{-4}$	[12]
18	$2.364 \times 10^{-9}$	$2.30(0.30) \times 10^{-9}$	[13]
28	$1.534 \times 10^{-10}$	$1.561(0.016) \times 10^{-10}$	[17]
35	$3.937 \times 10^{-11}$	$3.932(0.032) \times 10^{-11}$	[18]
36	$3.320 \times 10^{-11}$	$3.408(0.034) \times 10^{-11}$	[14]
41	$1.514 \times 10^{-11}$	$1.533(0.060) \times 10^{-11}$	[19]

TABLE IV. Two-photon decay rates ( $s^{-1}$ ) for  $2^1S_0$  and  $2^3S_1$  states of heliumlike ions are compared with the previous theoretical values. Drake [7] values include estimated relativistic corrections. Numbers in brackets represent powers of ten.

$Z$	$2^1S_0$ rates	Drake [7]	$2^3S_1$ rates	Drake <i>et al.</i> [5]	Bely and Faucher [9]
2	5.102[01]	5.094[01]	3.17[-9]	4.02[-9]	3.47[-9]
3	1.940[03]	1.938[03]	1.25[-6]	1.50[-6]	
4	1.816[04]	1.815[04]	5.53[-5]	6.36[-5]	
5	9.211[04]	9.202[04]	8.93[-4]	10.1[-4]	8.36[-4]
6	3.300[05]	3.296[05]	8.05[-3]	8.93[-3]	
7	9.444[05]	9.537[05]	4.95[-2]	5.44[-2]	
8	2.310[06]	2.306[06]	2.33[-1]	2.54[-1]	2.23[-1]
9	5.029[06]	5.021[06]	8.94[-1]	9.73[-1]	
10	1.001[07]	0.999[07]	2.95[00]	3.20[00]	
12	3.249[07]	3.242[07]	2.26[01]		2.19[01]
16	2.020[08]	2.014[08]	5.33[02]		5.09[02]

distributions for  $Z=20$  are slightly, but noticeably, different and this difference grows as  $Z$  decreases.

Total two-photon decay rates for  $2^3S_1$  state are presented in Table V. These rates are a factor of  $10^4$  smaller than the  $M1$  decay rates [24] for the entire isoelectronic sequence. It is worth noting that the corresponding hydrogenic transition  $2s_{1/2} \rightarrow 1s_{1/2}$  exhibits a different evolution of competing  $2E1$  and  $M1$  branches [26]. The  $2E1$  branch dominates for hydrogenic ions with nuclear charges below  $Z \approx 50$  while the  $M1$  rate dominates for larger  $Z$ . In Table IV, we give a comparison of decay rates for  $2^3S_1$  states of heliumlike ions with the previous theoretical values of Drake *et al.* [5] and Bely and Faucher [9]. We notice a significant discrepancy with the present values, especially for small nuclear charges. This inconsistency is due to cancellation effects in the  $2^3S_1$  case. The probable reason [27] for most of the discrepancy in the low- $Z$  range is a small spin-dependent mixing of the  $1^1S_0$  final state with doubly excited  $(pp')^3P_0$  states, which was not included in the nonrelativistic calculations of Drake, Victor, and Dalgarno [5] for the two-photon decay rate. The effect of this mixing, however, has been calculated for the single photon  $2^3P_1-1^1S_0$  intercombination transition [28], where it produces a small decrease in the decay rate. The relative effect of the additional terms decreases in proportion to  $1/Z$  with increasing  $Z$  in accord with the present results.

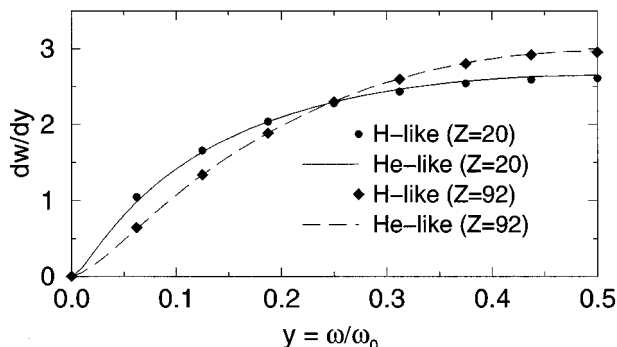


FIG. 5. Comparison of the photon energy distributions of  $2^1S_0$  decay with the corresponding hydrogenic  $2s_{1/2} \rightarrow 1s_{1/2}$  energy distributions for  $Z=20$  and  $Z=92$ .

We present the  $2^3S_1$  photon energy distributions for  $Z < 40$  in the upper panel of Fig. 6 and for  $Z > 40$  in the lower panel. Similar to the  $2^1S_0$  case, the  $Z$  dependence of the photon energy distribution is not monotonic;  $Z \approx 30$  is a minimum of the reduced FWHM considered as a function of  $Z$ . This nonmonotonic behavior is shown in the lower panel of Fig. 7. The value of  $y = \omega/\omega_0$  at the maximum of the energy distribution,  $y_{\max}$ , is shown as a function of  $Z$  in the upper panel of Fig. 7.

In the present calculations, we have employed a consistent approach of using theoretical energies from the relativistic CI energy calculations. These energies include both Coulomb and Breit interactions, but do not include radiative corrections. The practice of scaling single-photon rates to the experimental (or more accurate [29]) energies,  $\omega_{\text{expt}}$ , would result in an additional factor of  $(\omega_{\text{expt}}/\omega_0)^7$ . Such scaling gives corrections that are negligible for small  $Z$ , but increase

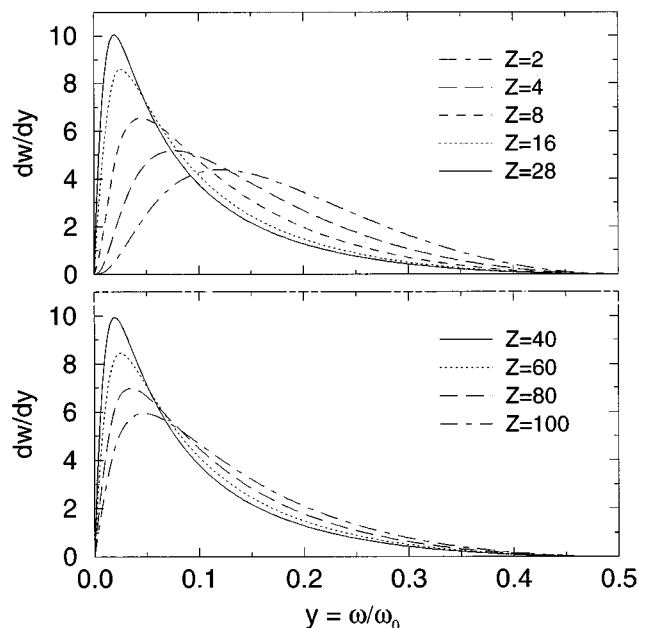


FIG. 6. Left branch of the  $2^3S_1$  distribution functions  $dw/dy$ , normalized to area 2, as in Fig. 1. The upper panel gives  $dw/dy$  for  $Z < 30$  and the lower panel gives results for  $Z > 30$ .

TABLE V. Two-photon decay rates  $w_{2\gamma}$  for  $2^3S_1$  states of heliumlike ions. Numbers in brackets represent powers of ten.

$Z$	$w_{2\gamma}$ ( $s^{-1}$ )	$Z$	$w_{2\gamma}$ ( $s^{-1}$ )
2	3.17[-9]	30	4.17[05]
3	1.25[-6]	35	2.01[06]
4	5.53[-5]	36	2.67[06]
5	8.93[-4]	40	7.69[06]
6	8.05[-3]	41	9.82[06]
7	4.95[-2]	45	2.46[07]
8	2.33[-1]	50	6.88[07]
9	8.94[-1]	54	1.44[08]
10	2.95[00]	55	1.72[08]
11	8.59[00]	60	3.93[08]
12	2.26[01]	65	8.34[08]
13	5.49[01]	70	1.66[09]
14	1.24[02]	75	3.14[09]
15	2.64[02]	80	5.65[09]
16	5.33[02]	82	7.07[09]
17	1.03[03]	85	9.78[09]
18	1.91[03]	90	1.63[10]
19	3.41[03]	92	1.98[10]
20	5.91[03]	95	2.64[10]
25	6.27[04]	100	4.15[10]
28	2.04[05]		

with  $Z$  up to a level of about 1% at  $Z=100$ .

In summary, we have performed *ab initio* relativistic calculations of two-photon decay rates and photon energy distributions of metastable  $2^1S_0$  and  $2^3S_1$  states for heliumlike ions with nuclear charges in the range  $Z = 2-100$ . The data presented for  $2^1S_0$  decay rates are in good agreement with

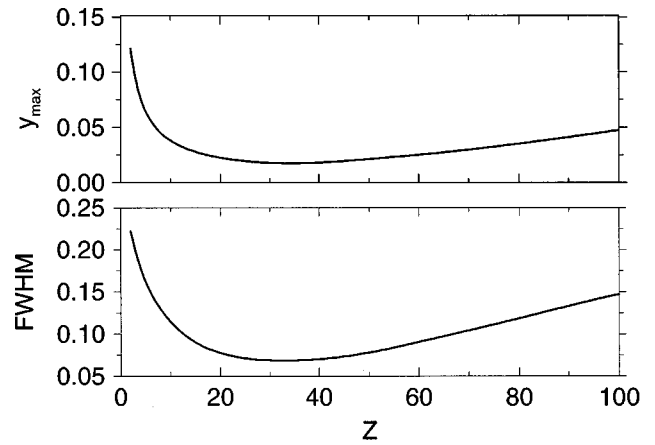


FIG. 7. The reduced full width at half maximum (FWHM) of the left branches of the two-photon energy distributions  $dw/dy$  for the  $2^3S_1$  state shown in Fig. 6 is plotted as a function of nuclear charge  $Z$  in the lower panel. The value of  $y = \omega/\omega_0$  at the maximum point of the distributions,  $y_{\max}$ , is plotted in the upper panel.

the available experimental values and with estimates of relativistic corrections by Drake [7]. We also find that the  $2^3S_1$  two-photon rates are smaller than the corresponding single-photon  $M1$  decay rates by a factor of about  $10^{-4}$  throughout the entire helium isoelectronic sequence.

#### ACKNOWLEDGMENTS

This work was supported in part by NSF Grant No. PHY 95-13179. The authors owe thanks to A. E. Livingston, H. G. Berry, and R. W. Dunford for valuable comments and suggestions on this work. Thanks are also due to K. T. Cheng for help on extrapolation of the partial-wave sequence.

- 
- [1] A. Dalgarno, Mon. Not. R. Astron. Soc. **131**, 311 (1966).  
[2] A. Dalgarno and G. A. Victor, Proc. Phys. Soc. London **87**, 371 (1966).  
[3] G. A. Victor, Proc. Phys. Soc. London **91**, 825 (1967).  
[4] G. A. Victor and A. Dalgarno, Phys. Rev. Lett. **18**, 1105 (1967).  
[5] G. W. F. Drake, G. A. Victor, and A. Dalgarno, Phys. Rev. **186**, 25 (1969).  
[6] V. Jacobs, Phys. Rev. A **4**, 939 (1971).  
[7] G. W. F. Drake, Phys. Rev. A **34**, 2871 (1986).  
[8] O. Bely, J. Phys. B **1**, 718 (1968).  
[9] O. Bely and P. Faucher, Astron. Astrophys. **1**, 37 (1969).  
[10] G. W. F. Drake and A. Dalgarno, Astrophys. J. **151**, L121 (1968).  
[11] R. S. vanDyck, Jr., C. E. Johnson, and H. S. Shugart, Phys. Rev. A **4**, 1327 (1971).  
[12] M. H. Prior and H. A. Shugart, Phys. Rev. Lett. **27**, 902 (1971).  
[13] R. Marrus and R. W. Schmieder, Phys. Rev. A **5**, 1160 (1972).  
[14] R. Marrus, V. S. Vicente, P. Charles, J. P. Briand, F. Bosch, D. Liesen, and I. Varga, Phys. Rev. Lett. **56**, 1683 (1986).  
[15] R. W. Dunford, H. G. Berry, K. O. Groenveld, M. Hass, E. Bakke, M. L. A. Raphaelian, A. E. Livingston, and L. J. Curtis, Phys. Rev. A **38**, 5423 (1988).  
[16] R. W. Dunford, M. Hass, E. Bakke, H. G. Berry, C. J. Liu, M. L. A. Raphaelian, and L. J. Curtis, Phys. Rev. Lett. **62**, 2809 (1989).  
[17] R. W. Dunford, H. G. Berry, D. A. Church, M. Hass, C. J. Liu, M. L. A. Raphaelian, B. J. Zabransky, L. J. Curtis, and A. E. Livingston, Phys. Rev. A **48**, 2729 (1993).  
[18] R. W. Dunford, H. G. Berry, S. Cheng, E. P. Kanter, C. Kurtz, B. J. Zabransky, A. E. Livingston, and L. J. Curtis, Phys. Rev. A **48**, 1929 (1993).  
[19] A. Simionovici, B. B. Birkett, J. P. Briand, P. Charles, D. D. Dietrich, K. Finlayson, P. Indelicato, D. Liesen, and R. Marrus, Phys. Rev. A **48**, 1695 (1993).  
[20] R. Ali, I. Ahmad, H. G. Berry, R. W. Dunford, D. S. Gemmell, E. P. Kanter, P. H. Mokler, A. E. Livingston, S. Cheng, and L. J. Curtis, Nucl. Instrum. Methods Phys. Res. B **98**, 69 (1995).  
[21] R. Ali, I. Ahmad, R. W. Dunford, D. S. Gemmell, M. Jung, E. P. Kanter, P. H. Mokler, H. G. Berry, A. E. Livingston, S. Cheng, and L. J. Curtis, Phys. Rev. A **55**, 994 (1997).  
[22] M. H. Chen, K. T. Cheng, and W. R. Johnson, Phys. Rev. A

- 47, 3692 (1993).
- [23] K. T. Cheng, M. H. Chen, W. R. Johnson, and J. Sapirstein, *Phys. Rev. A* **50**, 247 (1994).
- [24] W. R. Johnson, D. R. Plante, and J. Sapirstein, in *Advances in Atomic, Molecular, and Optical Physics*, edited by B. Bederson and H. Walther (Addison-Wesley, New York, 1995), Vol. 35, pp. 255–329.
- [25] W. R. Johnson and K. T. Cheng, *Phys. Rev. A* **53**, 1375 (1996).
- [26] W. R. Johnson, *Phys. Rev. A* **29**, 1123 (1972).
- [27] G. W. F. Drake (private communication).
- [28] G. W. F. Drake, *J. Phys. B* **9**, L169 (1976).
- [29] D. R. Plante, Ph.D. thesis, University of Notre Dame, 1995 (unpublished).